A NEW DISCONTINUOUS GALERKIN FORMULATION FOR WAVE EQUATIONS IN SECOND ORDER FORM

DANIEL APPELÖ* AND THOMAS HAGSTROM†

Abstract. We develop and analyze a new strategy for the spatial discontinuous Galerkin discretization of wave equations in second order form. The method features a direct, mesh-independent approach to defining interelement fluxes. Both energy-conserving and upwind discretizations can be devised. We derive a priori error estimates in the energy norm for certain fluxes and present numerical experiments showing that optimal convergence in L^2 is obtained.

Key words. discontinuous Galerkin, upwind flux, wave equation

AMS subject classifications. 65M12

1. Introduction. In recent years, discontinuous Galerkin methods have proven to be an effective approach to developing high-order, energy-stable discretizations of time-domain wave propagation problems in complex geometry. These developments encompass both first order hyperbolic systems [10, 13, 6, 7, 11, 15, 12] and wave equations in second order form [14, 9, 5]. Despite the fact that second order systems can often be rewritten in first order form via the introduction of new variables, the formulations for second order equations appear quite different. Energy-conserving methods include the symmetric interior penalty (SIPG) method of [9] and the local discontinuous Galerkin (LDG) method of [5]. Stability, in the first case, relies on the proper choice of internal penalty parameters (see also [1]). In the LDG method additional gradient variables are introduced and combined with an alternating flux. The nonsymmetric interior penalty method of [14], on the other hand, is dissipative with the dissipation again dependent on a proper choice of internal penalty parameters. Here we introduce a new formulation, which seems more naturally related to the first-order formulations, which can be either energy-conserving or energy-dissipating depending on a simple choice of the numerical flux. It bears similarities to the LDG method of [5], but instead of spatial gradients we introduce the time derivatives as new unknowns. Besides requiring fewer dependent variables than LDG, we believe the method has a number of other attractive properties. First, it admits a wide variety of mesh-independent flux choices naturally associated with the energy flux, including a simple upwinding strategy based on flux splitting. We are particularly interested in upwind schemes, not only due to their optimal convergence, but for the robust stability properties they possess. This seems particularly attractive for their use on hybrid grids, as carried out for first order systems in [4], and for nonlinear problems. We also find that their convergence profiles are more regular than those observed for the energy-conserving schemes. Second, we observe experimentally optimal convergence in both the L^2 and energy norms for a variety of flux choices, including both dissipative and nondissipative examples, without the need to construct special projections of the initial data. The optimal convergence in the energy norm is proven in one space dimension. Finally, we note that the proposed discretization arises naturally from a general formulation based directly on the Lagrangian, which is central to the formulation of wave equations in most physical settings.

The outline of the paper is as follows. In Section 2 we explain the formulation for general linear wave equations and prove the basic energy identity for a wide choice of fluxes. In Section 3 we specialize to the scalar wave equation. For that case we derive error estimates in the energy norm for all flux choices considered. Optimal convergence is proven in one space dimension for flux parameters satisfying a certain algebraic relation, which covers both the energy-conserving alternating flux and the dissipative upwind Sommerfeld flux. Simple numerical experiments with the scalar wave equation in Section 4 lead to the observation that the convergence in L^2 is one order higher than in the energy norm, and that optimal convergence with the alternating or upwind flux is maintained for a non-Cartesian grid of quadrilaterals. We also experiment with changing the relative degrees of the approximation to the solution and the time derivative, with the conclusion that increasing the order of approximation of the time derivative from the value needed for optimal convergence is generally not

*Department of Mathematics and Statistics, University of New Mexico, 1 University of New Mexico, Albuquerque, NM 87131. appelo@unm.edu. Supported in part by NSF Grant DMS-1319054. Any conclusions or recommendations expressed in this paper are those of the author and do not necessarily reflect the views NSF.

†Department of Mathematics, Southern Methodist University, PO Box 750156, Dallas, TX 75275-0156, thagstrom@smu.edu. Supported in part by ARO Contract W911NF-09-1-0344 and NSF Grants OCI-0904773, DMS-1418871. Any conclusions or recommendations expressed in this paper are those of the author and do not necessarily reflect the views of ARO or NSF.

useful, and for some fluxes detrimental. An exception is the case of the central flux, where an improved order of convergence for the solution, but not the time derivative, was observed. Lastly we mention our ongoing work to extend the method to problems with discontinuous coefficients and nonlinearities.

2. General Formulation. We consider, in general, wave equations associated with a nonnegative energy functional or Hamiltonian

$$E(t) = \int_\Omega \frac{1}{2} \left| \frac{\partial \mathbf{u}}{\partial t} \right|^2 + G(\mathbf{u}, \nabla \mathbf{u}, \mathbf{x}). \tag{2.1}$$

Here $\Omega \subset \mathbb{R}^d$, $\mathbf{u}(\mathbf{x}, t) \in \mathbb{R}^m$. The system of wave equations we aim to solve, which can be identified as the Euler-Lagrange equations derived from the action principle associated with the Lagrangian $\frac{1}{2} \left| \frac{\partial \mathbf{u}}{\partial t} \right|^2 - G - \mathbf{u} \cdot \mathbf{f}$ [16], is given by

$$\frac{\partial^2 u_i}{\partial t^2} = \sum_k \frac{\partial}{\partial x_k} \left(\frac{\partial G}{\partial u_{i,k}} \right) - \frac{\partial G}{\partial u_i} + f_i, \tag{2.2}$$

where we define $u_{i,k} = \frac{\partial u_i}{\partial x_k}$. Then introducing as a new variable, $v_i = \frac{\partial u_i}{\partial t}$, we find that the change of energy on an element Ω_j is given by the source term and a boundary contribution

$$\frac{d}{dt} \int_{\Omega_j} \frac{1}{2} |\mathbf{v}|^2 + G = \int_{\Omega_j} \mathbf{v} \cdot \mathbf{f} + \int_{\partial \Omega_j} \sum_{i,k} v_i \frac{\partial G}{\partial u_{i,k}} n_k, . \tag{2.3}$$

where $\mathbf{n}$ denotes the outward unit normal.

To discretize on a simplicial element we require that the components of $(\mathbf{u}^h, \mathbf{v}^h)$ restricted to Ω_j be polynomials of degree s and q respectively; that is elements of $(\Pi^s)^m \times (\Pi^q)^m$. Typically, as discussed in Remark 1, we choose $s = q + 1$ corresponding to the role of v_i^h as an approximate derivative of u_i^h, but the stability theory allows independent choice of approximation spaces. On quadrilateral/hexahedral elements these spaces would be replaced by the corresponding spaces of tensor product polynomials: $(\mathbb{Q}^s)^m \times (\mathbb{Q}^q)^m$.

Now specialize to the linear case; that is, assume that G depends quadratically on $\mathbf{u}$ and $\nabla \mathbf{u}$:

$$G = \sum_{i,j,k,l} g^{(2)}_{(i,k),(j,l)}(\mathbf{x}) u_{i,k} u_{j,l} + \sum_{i,j,k} g^{(1)}_{(i,k),j}(\mathbf{x}) u_{i,k} u_j + \sum_{i,j} g^{(0)}_{ij} u_i u_j \equiv w^T g w, \tag{2.4}$$

where w denotes an $m(d+1)$-dimensional vector containing the $u_{i,k}$, u_i and g is an $m(d+1) \times m(d+1)$ symmetric positive semi-definite matrix containing the $g^{(j)}$. We seek approximations to the system

$$\frac{\partial u_i}{\partial t} - v_i = 0, \tag{2.5}$$

$$\frac{\partial v_i}{\partial t} - \sum_k \frac{\partial}{\partial x_k} \left(\frac{\partial G}{\partial u_{i,k}} \right) + \frac{\partial G}{\partial u_i} = f_i, \tag{2.6}$$

satisfying a discrete energy identity analogous to (2.3). To motivate our choice consider the discrete energy in Ω_j:

$$E_j^h(t) = \int_{\Omega_j} \frac{1}{2} \left| \mathbf{v}^h \right|^2 + G(\mathbf{u}^h, \nabla \mathbf{u}^h, \mathbf{x}) \tag{2.7}$$

and its time derivative

$$\frac{dE_j^h}{dt} = \sum_i \int_{\Omega_j} v_i^h \frac{\partial v_i^h}{\partial t} + \sum_k \frac{\partial G}{\partial u_{i,k}} \frac{\partial^2 u_i^h}{\partial x_k \partial t} + \frac{\partial G}{\partial u_i} \frac{\partial u_i^h}{\partial t}. \tag{2.8}$$

To develop a weak form compatible with the discrete energy we test (2.5) with $-\sum_k \frac{\partial}{\partial x_k} \frac{\partial G}{\partial u_{i,k}}(\phi_u, \nabla \phi_u, \mathbf{x}) + \frac{\partial G}{\partial u_i}(\phi_u, \nabla \phi_u, \mathbf{x})$, $\phi_u \in (\Pi^s)^m$ and (2.6) by $\phi_{v,i} \in \Pi^q$. In addition, as in the construction of discontinuous

Galerkin methods for first order symmetric hyperbolic systems, where the energy is simply the L^2-norm, we impose corrections based on boundary states to be specified later

$$v_i^* \approx v_i, \qquad w_{i,k}^* \approx \frac{\partial G}{\partial u_{i,k}}. \tag{2.9}$$

This results in the equations for $i = 1, \ldots, m$:

$$\int_{\Omega_j} \left(-\sum_k \frac{\partial}{\partial x_k} \frac{\partial G}{\partial u_{i,k}}(\phi_u, \nabla\phi_u, \mathbf{x}) + \frac{\partial G}{\partial u_i}(\phi_u, \nabla\phi_u, \mathbf{x}) \right) \left(\frac{\partial u_i^h}{\partial t} - v_i^h \right) = \int_{\partial\Omega_j} \sum_k n_k \frac{\partial G}{\partial u_{i,k}}(\phi_u, \nabla\phi_u, \mathbf{x}) \left(v_i^* - \frac{\partial u_i^h}{\partial t} \right), \tag{2.10}$$

$$\int_{\Omega_j} \phi_{v,i} \frac{\partial v_i^h}{\partial t} + \phi_{v,i} \left(-\sum_k \frac{\partial}{\partial x_k} \frac{\partial G}{\partial u_{i,k}}(\mathbf{u}^h, \nabla\mathbf{u}^h, \mathbf{x}) + \frac{\partial G}{\partial u_i}(\mathbf{u}^h, \nabla\mathbf{u}^h, \mathbf{x}) \right) - \phi_{v,i} f_i(\mathbf{x}, t) = \int_{\partial\Omega_j} \phi_{v,i} \sum_k n_k \left(w_{i,k}^* - \frac{\partial G}{\partial u_{i,k}}(\mathbf{u}^h, \nabla\mathbf{u}^h, \mathbf{x}) \right). \tag{2.11}$$

In what follows it is useful to note that an integration by parts in (2.10)-(2.11) yields the alternative form

$$\int_{\Omega_j} \left(\sum_k \frac{\partial G}{\partial u_{i,k}}(\phi_u, \nabla\phi_u, \mathbf{x}) \frac{\partial}{\partial x_k} + \frac{\partial G}{\partial u_i}(\phi_u, \nabla\phi_u, \mathbf{x}) \right) \left(\frac{\partial u_i^h}{\partial t} - v_i^h \right) = \int_{\partial\Omega_j} \sum_k n_k \frac{\partial G}{\partial u_{i,k}}(\phi_u, \nabla\phi_u, \mathbf{x}) \left(v_i^* - v_i^h \right), \tag{2.12}$$

$$\int_{\Omega_j} \phi_{v,i} \frac{\partial v_i^h}{\partial t} + \sum_k \frac{\partial \phi_{v,i}}{\partial x_k} \frac{\partial G}{\partial u_{i,k}}(\mathbf{u}^h, \nabla\mathbf{u}^h, \mathbf{x}) + \phi_{v,i} \frac{\partial G}{\partial u_i}(\mathbf{u}^h, \nabla\mathbf{u}^h, \mathbf{x}) - \phi_{v,i} f_i(\mathbf{x}, t) = \int_{\partial\Omega_j} \sum_k n_k \phi_{v,i} w_{i,k}^*. \tag{2.13}$$

Although, by construction, solutions of (2.10)-(2.11) or (2.12)-(2.13) will satisfy an energy identity made precise in Theorem 1 below, these equations are often insufficient to uniquely determine the time derivatives within an element. In particular, in many cases G is invariant with respect to certain transformations of $\mathbf{u}$. Assume that these transformations are independent of $\mathbf{x}$. In the linear case the transformations are generated by null vectors, $u_{i,k} = \frac{\partial \tilde{\phi}_{u,i}}{\partial x_k}$, $u_i = \tilde{\phi}_{u,i}$ of the matrix, g, introduced in (2.4). We assume these null vectors are elements of $(\Pi^s)^m$. Then equation (2.10) or (2.12) does not determine the projection of $\frac{\partial \mathbf{u}^h}{\partial t}$ onto this null space, so we supplement it by

$$\sum_i \int_{\Omega_j} \tilde{\phi}_{u,i} \left(\frac{\partial u_i^h}{\partial t} - v_i^h \right) = 0, \tag{2.14}$$

for all null vectors, $\tilde{\phi}_u$, of g. In what follows we denote by $\mathcal{N}$ the null space of g.

In summary, define $\mathcal{P}^{s,q,m}$ to be the set of all functions $U^h = (u^h, v^h)$ whose restriction to an element Ω_j is an element of $(\Pi^s)^m \times (\Pi^q)^m$. Then for $\Phi = (\phi_u, \phi_v, \tilde{\phi}_u) \in \mathcal{P}^{s,q,m} \times \mathcal{N}$ define:

$$\begin{aligned} \mathcal{B}(\Phi, U^h) \equiv & \sum_{i,j} \int_{\Omega_j} \left(\sum_k \frac{\partial G}{\partial u_{i,k}}(\phi_u, \nabla\phi_u, \mathbf{x}) \frac{\partial}{\partial x_k} + \frac{\partial G}{\partial u_i}(\phi_u, \nabla\phi_u, \mathbf{x}) + \tilde{\phi}_{u,i} \right) \left(\frac{\partial u_i^h}{\partial t} - v_i^h \right) \\ & + \sum_{i,j} \int_{\Omega_j} \phi_{v,i} \frac{\partial v_i^h}{\partial t} + \sum_k \frac{\partial \phi_{v,i}}{\partial x_k} \frac{\partial G}{\partial u_{i,k}}(\mathbf{u}^h, \nabla\mathbf{u}^h, \mathbf{x}) + \phi_{v,i} \frac{\partial G}{\partial u_i}(\mathbf{u}^h, \nabla\mathbf{u}^h, \mathbf{x}) \\ & - \sum_{i,j} \int_{\partial\Omega_j} \sum_k n_k \left(\frac{\partial G}{\partial u_{i,k}}(\phi_u, \nabla\phi_u, \mathbf{x}) \left(v_i^* - v_i^h \right) + \phi_{v,i} w_{i,k}^* \right). \end{aligned} \tag{2.15}$$

Introducing $\langle \cdot, \cdot \rangle$ to denote the standard L^2 inner product of vector-valued functions, we have the following succinct description of the semidiscrete problem.

PROBLEM 1. *Find $U^h \in \mathcal{P}^{s,q,m}$ such that for all $\Phi \in \mathcal{P}^{s,q,m} \times \mathcal{N}$*

$$\mathcal{B}(\Phi, U^h) = \langle \phi_v, \mathbf{f} \rangle.$$

We then have the following basic result.

THEOREM 1. *Suppose $U^h(t)$ and the fluxes $\mathbf{v}^*$, $\mathbf{w}^*$ are given. Suppose further that (2.2) is linear. Then $\frac{dU^h}{dt}$ satisfying Problem 1 is uniquely determined and the energy identity for $E^h(t) = \sum_j E^h_j(t)$*

$$\frac{dE^h}{dt} = \sum_{i,j} \int_{\Omega_j} v_i^h f_i(\mathbf{x}, t) + \sum_{i,j} \int_{\partial\Omega_j} \left(\sum_k n_k \left(v_i^* - v_i^h \right) \frac{\partial G}{\partial u_{i,k}}(\mathbf{u}^h, \nabla \mathbf{u}^h, \mathbf{x}) + v_i^h w_{i,k}^* \right), \tag{2.16}$$

is satisfied.

Proof: The system on the element Ω_j is linear in the time derivatives, and the mass matrix determining $\frac{\partial v_i^h}{\partial t}$ is obviously nonsingular. To show that $\frac{\partial \mathbf{u}^h}{\partial t}$ is uniquely determined we first note that the number of linear equations matches the dimensionality of $(\Pi^s)^m$; that is the dimension equals number of independent equations represented by (2.12) plus those represented by (2.14). Then if the data v_i^h, v_i^* vanishes in (2.12) we must have that $\frac{\partial \mathbf{u}^h}{\partial t} \in \mathcal{N}$ and by (2.14) is in fact $\mathbf{0}$. Setting $\Phi = (U^h, \mathbf{0})$ in Problem 1, equation (2.16) directly follows.

2.1. Fluxes. To complete the problem specification we must prescribe the states $\mathbf{w}^*$, $\mathbf{v}^*$ both at interelement and physical boundaries. Following the standard convention (e.g. [11]) let the superscripts "$\pm$" refer to traces of data from outside and inside the element respectively. Moreover we introduce the notation

$$\{\{v_i\}\} = \frac{1}{2}\left(v_i^+ + v_i^-\right), \quad [[v_i]] = v_i^+ \mathbf{n}^+ + v_i^- \mathbf{n}^-, \tag{2.17}$$

$$\{\{\frac{\partial G}{\partial u_{i,k}}\}\} = \frac{1}{2}\left(\frac{\partial G}{\partial u_{i,k}}(\mathbf{u}^+, \nabla \mathbf{u}^+, \mathbf{x}) + \frac{\partial G}{\partial u_{i,k}}(\mathbf{u}^-, \nabla \mathbf{u}^-, \mathbf{x}) \right), \tag{2.18}$$

$$[[D_{\nabla u_i} G]] = \sum_k \left(\frac{\partial G}{\partial u_{i,k}}(\mathbf{u}^+, \nabla \mathbf{u}^+, \mathbf{x}) n_k^+ + \frac{\partial G}{\partial u_{i,k}}(\mathbf{u}^-, \nabla \mathbf{u}^-, \mathbf{x}) n_k^- \right). \tag{2.19}$$

Focus first on the interelement boundaries. For definiteness label two elements sharing a boundary by 1 and 2. Then their net contribution to the energy derivative is the integral of

$$J^h = \sum_{i,k} \left(v_i^* - v_{i,1}^h \right) \frac{\partial G}{\partial u_{i,k}}(\mathbf{u}_1^h, \nabla \mathbf{u}_1^h, \mathbf{x}) n_k^{(1)} + \left(v_i^* - v_{i,2}^h \right) \frac{\partial G}{\partial u_{i,k}}(\mathbf{u}_2^h, \nabla \mathbf{u}_2^h, \mathbf{x}) n_k^{(2)} + \left(v_{i,1}^h n_k^{(1)} + v_{i,2}^h n_k^{(2)} \right) w_{i,k}^*. \tag{2.20}$$

Energy conserving methods follow from choices which enforce $J^h = 0$. Simple examples are the **central flux**

$$v_i^* = \{\{v_i^h\}\}, \quad w_{i,k}^* = \{\{\frac{\partial G^h}{\partial u_{i,k}}\}\}, \tag{2.21}$$

or the **alternating flux**

$$v_i^* = v_{i,1}^h, \quad w_{i,k}^* = \frac{\partial G}{\partial u_{i,k}}(\mathbf{u}_2^h, \nabla \mathbf{u}_2^h, \mathbf{x}). \tag{2.22}$$

To define upwind fluxes, which will lead to $J^h < 0$ in the presence of jumps, we introduce a flux splitting determined by a parameter $\zeta_i > 0$:

$$\sum_k v_i \frac{\partial G}{\partial u_{i,k}} n_k = \frac{1}{4\zeta_i} \left(v_i + \zeta_i \sum_k \frac{\partial G}{\partial u_{i,k}} n_k \right)^2 - \frac{1}{4\zeta_i} \left(v_i - \zeta_i \sum_k \frac{\partial G}{\partial u_{i,k}} n_k \right)^2 \equiv F_i^+ - F_i^-, \tag{2.23}$$

and choose the boundary states so that F_i^+ is computed using values from outside the element and F_i^- using the values from inside. That is we enforce the equations for $\ell = 1, 2$:

$$v_i^* - \zeta_i \sum_k w_{i,k}^* n_k^{(\ell)} = v_{i,\ell}^h - \zeta_i \sum_k \frac{\partial G}{\partial u_{i,k}}(\mathbf{u}_\ell^h, \nabla \mathbf{u}_\ell^h, \mathbf{x}) n_k^{(\ell)}. \tag{2.24}$$

This leads to what we call the **Sommerfeld flux**

$$v_i^* = \{\{v_i^h\}\} - \frac{\zeta_i}{2}[[D_{\nabla u_i} G^h]], \tag{2.25}$$

$$w_{i,k}^* = -\frac{1}{2\zeta_i}[[v_i^h]]_k + \{\{\frac{\partial G^h}{\partial u_{i,k}}\}\}. \tag{2.26}$$

For the Sommerfeld flux we find

$$J^h = -\frac{1}{2}\sum_i \left[\frac{1}{\zeta_i} \mid [[v_i^h]] \mid^2 + \zeta_i [[D_{\nabla u_i} G^h]]^2\right]. \tag{2.27}$$

Lastly we note that we can use various combinations of the fluxes described above. One general parametrization is given by

$$v_i^* = \left(\alpha_i v_{i,1}^h + (1-\alpha_i) v_{i,2}^h\right) - \tau_i [[D_{\nabla u_i} G^h]], \tag{2.28}$$

$$w_{i,k}^* = -\beta_i [[v_i^h]]_k + \left((1-\alpha_i)\frac{\partial G}{\partial u_{i,k}}(\mathbf{u}_1^h, \nabla \mathbf{u}_1^h, \mathbf{x}) + \alpha_i \frac{\partial G}{\partial u_{i,k}}(\mathbf{u}_2^h, \nabla \mathbf{u}_2^h, \mathbf{x})\right). \tag{2.29}$$

For the general case we find

$$J^h = -\sum_i \left[\beta_i \mid [[v_i^h]] \mid^2 + \tau_i [[D_{\nabla u_i} G^h]]^2\right]. \tag{2.30}$$

The previous cases correspond to:
Central flux : $\alpha_i = 1/2$, $\beta_i = \tau_i = 0$.
Alternating flux : $\alpha_i = 0, 1$, $\beta_i = \tau_i = 0$.
Sommerfeld flux : $\alpha_i = 1/2$, $\beta_i = \frac{1}{2\zeta_i}$, $\tau_i = \frac{\zeta_i}{2}$.

2.2. Boundary conditions. Lastly we consider the approximation of boundary conditions. Precisely, for $\mathbf{x} \in \partial\Omega$ we suppose the boundary condition takes the form

$$a_i(\mathbf{x})\frac{\partial u_i}{\partial t} + b_i(\mathbf{x}) \sum_k n_k \frac{\partial G}{\partial u_{i,k}}(\mathbf{u}, \nabla \mathbf{u}, \mathbf{x}) = 0, \tag{2.31}$$

where $a_i^2 + b_i^2 = 1$, $a_i, b_i \geq 0$. Note that Dirichlet conditions correspond to $a_i = 1$, $b_i = 0$, and Neumann conditions to $a_i = 0$, $b_i = 1$. More general boundary conditions are possible, but their treatment would be more complex.

With these boundary conditions a complete energy identity can be obtained. In particular the energy flux through the boundary is nonpositive

$$\begin{aligned} S &= \int_{\partial\Omega} \sum_i \left(\frac{\partial u_i}{\partial t} \cdot \sum_k n_k \frac{\partial G}{\partial u_{i,k}}\right) \\ &= -\int_{\partial\Omega} \sum_i a_i b_i \left(\left(\frac{\partial u_i}{\partial t}\right)^2 + \left(\sum_k n_k \frac{\partial G}{\partial u_{i,k}}\right)^2\right) \leq 0. \end{aligned} \tag{2.32}$$

To approximate the boundary condition we choose v_i^*, $w_{i,k}^*$ to be consistent with (2.31):

$$a_i v_i^* + b_i \sum_k n_k w_{i,k}^* = 0, \tag{2.33}$$

and insist that the starred states match the interior states if the interior states satisfy the boundary condition. That is, all jumps must be proportional to

$$\rho_i = a_i(\mathbf{x})v_i^h + b_i(\mathbf{x})\sum_k n_k \frac{\partial G}{\partial u_{i,k}}(\mathbf{u}^h, \nabla \mathbf{u}^h \mathbf{x}). \tag{2.34}$$

Taking into account (2.33) we find a one parameter family of consistent choices:

$$v_i^* = v_i - (a_i - \eta_i b_i)\rho_i \tag{2.35}$$

$$w_{i,k}^* = \frac{\partial G}{\partial u_{i,k}} - n_k(b_i + \eta_i a_i)\rho_i. \tag{2.36}$$

Then the discrete energy flux is given by

$$S^h = -\int_{\partial\Omega}\sum_i \left[a_i b_i \left((v_i^*)^2 + \left(\sum_k n_k w_{i,k}^* \right)^2 \right) + \rho_i^2 \left((1-\eta_i^2)a_i b_i + \eta_i(a_i^2 - b_i^2) \right) \right]. \tag{2.37}$$

which will lead to a discrete energy estimate so long as

$$\gamma_i \equiv (1-\eta_i^2)a_i b_i + \eta_i(a_i^2 - b_i^2) \geq 0. \tag{2.38}$$

It is of interest to consider various special cases related to the choices of interior fluxes. A Sommerfeld flux follows from enforcing $v_i^* - \zeta_i \sum_k n_k w_{i,k}^* = v_i - \zeta_i \sum_k n_k \frac{\partial G}{\partial u_{i,k}}$ which implies

$$\eta_i = \frac{a_i - \zeta_i b_i}{\zeta_i a_i + b_i}, \quad \gamma_i = \frac{\zeta_i}{(\zeta_i a_i + b_i)^2} > 0. \tag{2.39}$$

In the case of Dirichlet or Neumann boundary conditions, which are energy-conserving for the continuous problem, we can enforce zero energy flux by choosing $\eta_i = 0$, a choice which satisfies (2.38) in all cases.

Finally combining (2.16), (2.30), and (2.37) we have the following discrete energy equality. Note that by F_j we denote interelement boundaries and by B_j element boundaries on $\partial\Omega_j$. Note that the identities do not require that the mesh is geometrically conformal.

THEOREM 2. *The discrete energy $E^h(t) = \sum_j E_j^h(t)$ with $E_j^h(t)$ defined in (2.7) satisfies*

$$\begin{aligned} \frac{dE^h}{dt} = &\sum_{i,j}\int_{\Omega_j} v_i^h f_i(\mathbf{x},t) \\ &- \sum_{i,j}\int_{F_j} \left[\beta_i |[[v_i^h]]|^2 + \tau_i [[D_{\nabla u_i} G^h]]^2 \right] \\ &- \sum_{i,j}\int_{B_j} \left[a_i b_i \left((v_i^*)^2 + \left(\sum_k n_k w_{i,k}^* \right)^2 \right) + \gamma_i \rho_i^2 \right]. \end{aligned} \tag{2.40}$$

Obviuously, if the flux parameters τ_i, β_i, γ_i are nonnegative and $\mathbf{f} = \mathbf{0}$ then $\frac{dE^h}{dt} \leq 0$, and if any are positive energy is dissipated even for energy-conserving boundary conditions.

3. Specialization to the scalar wave equation. To illustrate the general formulation and prepare for the detailed analysis that follows we specialize to the scalar wave equation with a smooth velocity. Now $m = 1$ and

$$G = \frac{c^2(\mathbf{x})}{2}|\nabla u|^2. \tag{3.1}$$

Here G is unchanged by the addition of a constant to u and therefore $\mathcal{N}$ consists of the piecewise constant functions $\tilde{\phi}_u$. Thus (2.14) becomes

$$\int_{\Omega_j} \frac{\partial u^h}{\partial t} - v^h = 0. \tag{3.2}$$

The form $\mathcal{B}$ is then given by

$$\begin{aligned}\mathcal{B}(\Phi, U^h) \equiv \sum_j \int_{\Omega_j} \left(c^2 \nabla \phi_u \cdot \nabla + \tilde{\phi}_u\right)\left(\frac{\partial u^h}{\partial t} - v^h\right) + \phi_v \frac{\partial v^h}{\partial t} + c^2 \nabla \phi_v \cdot \nabla u^h \\ - \sum_j \int_{\partial \Omega_j} c^2 \frac{\partial \phi_u}{\partial n}\left(v^* - v^h\right) + \phi_v \mathbf{w}^* \cdot \mathbf{n}.\end{aligned} \tag{3.3}$$

3.1. Error estimates in the energy norm. To derive error estimates we impose restrictions on the degrees, (s, q), namely $s - 2 \leq q \leq s$. Define the errors by

$$e_u = u - u^h, \quad e_v = v - v^h, \tag{3.4}$$

and let

$$D^h = (e_u, e_v). \tag{3.5}$$

Note the fundamental Galerkin orthogonality relation

$$\mathcal{B}(\Phi, D^h) = 0, \quad \forall \Phi \in \mathcal{P}^{s,q} \times \mathcal{N}. \tag{3.6}$$

To proceed we follow the standard approach of comparing (u^h, v^h) to an arbitrary function $(\tilde{u}^h, \tilde{v}^h) \in \mathcal{P}^{s,q}$. Given $(\tilde{u}^h, \tilde{v}^h)$ we define the differences

$$\tilde{e}_u = \tilde{u}^h - u^h, \quad \tilde{e}_v = \tilde{v}^h - v^h, \quad \delta_u = \tilde{u}^h - u, \quad \delta_v = \tilde{v}^h - v, \tag{3.7}$$

and let

$$\tilde{D}^h = (\tilde{e}_u, \tilde{e}_v) \in \mathcal{P}^{s,q}, \quad \tilde{D}_0^h = (\tilde{e}_u, \tilde{e}_v, 0) \in \mathcal{P}^{s,q} \times \mathcal{N}, \quad \Delta^h = (\delta_u, \delta_v). \tag{3.8}$$

Then since $D^h = \tilde{D}^h - \Delta^h$ we have the error equation

$$\mathcal{B}(\tilde{D}_0^h, \tilde{D}^h) = \mathcal{B}(\tilde{D}_0^h, \Delta^h). \tag{3.9}$$

Lastly define the energy of $\tilde{D}^h$ by

$$\mathcal{E}^h = \frac{1}{2} \sum_j \int_{\Omega_j} \tilde{e}_v^2 + c^2 |\nabla \tilde{e}_u|^2. \tag{3.10}$$

Then repeating the arguments which led to Theorem 2 we derive in analogy to (2.40)

$$\begin{aligned}\frac{d\mathcal{E}^h}{dt} = \mathcal{B}(\tilde{D}_0^h, \Delta^h) - \sum_j \int_{F_j} \left[\beta \left|[[\tilde{e}_v]]\right|^2 + \tau c^2 [[\nabla \tilde{e}_u]]^2\right] \\ - \sum_j \int_{B_j} \left[ab\left((\tilde{e}_v^*)^2 + (\tilde{e}_{\mathbf{w}}^* \cdot \mathbf{n})^2\right) + \gamma \left(a\tilde{e}_v + bc \nabla \tilde{e}_u \cdot \mathbf{n}\right)^2\right].\end{aligned} \tag{3.11}$$

We must now choose $(\tilde{u}^h, \tilde{v}^h)$ to achieve an acceptable error estimate. Note that in what follows we will assume for simplicity that $(u^h, v^h) = (\tilde{u}^h, \tilde{v}^h)$ at $t = 0$, though we do not satisfy this condition in the numerical experiments. We begin with a general analysis applicable for all our flux choices and for unstructured grids. The results are suboptimal for the Sommerfeld and alternating flux, and we will follow up with a sharper estimate

for those choices restricted to one space dimension. In particular, on Ω_j we impose for all times t and all $(\phi_u, \phi_v) \in \mathcal{P}^{s,q}$:

$$\int_{\Omega_j} c^2 \nabla \phi_u \cdot \nabla \delta_u = \int_{\Omega_j} c^2 \phi_v \delta_v = \int_{\Omega_j} \delta_u = 0. \tag{3.12}$$

Again the solvability of the gradient projection equation for $\tilde{u}^h$ follows from a counting and uniqueness argument; thus $(\tilde{u}^h, \tilde{v}^h)$ are uniquely defined. We then have, after an integration by parts:

$$\begin{aligned} \mathcal{B}(\tilde{D}_0^h, \Delta^h) = &\sum_j \int_{\Omega_j} c^2 \nabla \tilde{e}_u \cdot \nabla \frac{\partial \delta_u}{\partial t} + c^2 \nabla^2 \tilde{e}_u \delta_v + \nabla c^2 \cdot \nabla \tilde{e}_u \delta_v + \tilde{e}_v \frac{\partial \delta_v}{\partial t} + c^2 \nabla \tilde{e}_v \cdot \nabla \delta_u \\ &- \sum_j \int_{\partial \Omega_j} c^2 \left(\nabla \tilde{e}_u \cdot \mathbf{n} \right) \delta_v^* - \tilde{e}_v \delta_{\mathbf{w}}^* \cdot \mathbf{n}. \end{aligned} \tag{3.13}$$

Since $s-2 \leq q \leq s$ volume integral terms involving $\nabla^2 \tilde{e}_u$ and $\nabla \tilde{e}_v$ vanish by (3.12). Combining the contributions from neighboring elements we then have

$$\begin{aligned} \mathcal{B}(\tilde{D}_0^h, \Delta^h) = &\sum_j \int_{\Omega_j} \nabla c^2 \cdot \nabla \tilde{e}_u \delta_v + \tilde{e}_v \frac{\partial \delta_v}{\partial t} \\ &- c^2 \sum_k \int_{F_k} [[\nabla \tilde{e}_u]] \delta_v^* + [[\tilde{e}_v]] \cdot \delta_{\mathbf{w}}^* - c^2 \sum_k \int_{B_k} \left(\nabla \tilde{e}_u \cdot \mathbf{n} \right) \delta_v^* + \tilde{e}_v \delta_{\mathbf{w}}^* \cdot \mathbf{n}. \end{aligned} \tag{3.14}$$

Here we have introduced the fluxes δ_v^*, $\delta_{\mathbf{w}}^*$ built from δ_u, δ_v according to the flux specification being analyzed. Using (3.11) and (3.13) we can prove basic error estimates in the energy norm. Note that in what follows C will be a number independent of the functions involved and independent of the element diameter h for a shape-regular mesh sequence; $\| \cdot \|$ is used to denote a Sobolev norm and $| \cdot |$ denotes the associated seminorm.

THEOREM 3. *Suppose $s-2 \leq q \leq s$ and let $\bar{q} = \min(s-1, q)$. Then there exist numbers C_0, C_1 depending only on s, q and the shape-regularity of the mesh such that for a smooth solution u and time T*

$$\begin{aligned} \|e_v(\cdot,T)\|^2_{L^2(\Omega)} + \|\nabla e_u(\cdot,T)\|^2_{L^2(\Omega)} \leq (C_0 + C_1 T) \max_{t \leq T} \Big[&h^{2\sigma} \left(|u(\cdot,t)|^2_{H^{\bar{q}+2}(\Omega)} + |v(\cdot,t)|^2_{H^{\bar{q}+1}(\Omega)} \right) \\ &+ h^{2q+2} \left| \frac{\partial v}{\partial t}(\cdot,t) \right|^2_{H^{q+1}(\Omega)} \Big], \end{aligned} \tag{3.15}$$

where

$$\sigma = \begin{cases} \bar{q}, & \beta, \tau, \gamma \geq 0, \\ \bar{q} + \frac{1}{2}, & \beta, \tau, \gamma > 0. \end{cases} \tag{3.16}$$

Proof: Noting the equivalence between the standard Sobolev norms and those defined by the weight c^2, we recall the basic results following from the Bramble-Hilbert lemma (e.g. [8, Thm. 4.1.3]) and inverse inequalities (e.g. [8, Thm. 3.2.6]):

$$\|\delta_v\|^2_{L^2(\Omega)} + \|\nabla \delta_u\|^2_{L^2(\Omega)} \leq C h^{2\bar{q}+2} \left(|u(\cdot,t)|^2_{H^{\bar{q}+2}(\Omega)} + |v(\cdot,t)|^2_{H^{\bar{q}+1}(\Omega)} \right), \tag{3.17}$$

$$\| \frac{\partial \delta_v}{\partial t} \|^2_{L^2(\Omega)} \leq C h^{2q+2} \left| \frac{\partial v(\cdot,t)}{\partial t} \right|^2_{H^{q+1}(\Omega)}, \tag{3.18}$$

$$\|\delta_v^*\|^2_{L^2(\partial\Omega_j)} + \|\delta_{\mathbf{w}}^* \cdot \mathbf{n}\|^2_{L^2(\partial\Omega_j)} \leq C h^{2\bar{q}+1} \left(|u(\cdot,t)|^2_{H^{\bar{q}+2}(\Omega_j)} + |v(\cdot,t)|^2_{H^{\bar{q}+1}(\Omega_j)} \right), \tag{3.19}$$

$$\|\tilde{e}_v\|^2_{L^2(\partial\Omega_j)} + \|\nabla\tilde{e}_u\cdot\mathbf{n}\|^2_{L^2(\partial\Omega_j)} \leq Ch^{-1}\left(\|\tilde{e}_v\|^2_{L^2(\Omega_j)} + \|\nabla\tilde{e}_u\|^2_{L^2(\Omega_j)}\right). \tag{3.20}$$

First consider the case where $\tau = 0$ or $\beta = 0$. Then we simply estimate using the non-positivity of the contributions to $\frac{d\mathcal{E}^h}{dt}$ from the physical boundaries, B_k, and apply the Cauchy-Schwarz inequality in tandem with (3.18), (3.19) and (3.20) to estimate the remaining contributions

$$\begin{aligned}\frac{d\mathcal{E}^h}{dt} &\leq C\sum_j \|\nabla\tilde{e}_u\|_{L^2(\Omega_j)}\|\delta_v\|_{L^2(\Omega_j)} + \|\tilde{e}_v\|_{L^2(\Omega_j)}\|\frac{\partial\delta_v}{\partial t}\|_{L^2(\Omega_j)}\\ &\quad + C\sum_j \|\nabla\tilde{e}_u\|_{L^2(\partial\Omega_j)}\|\delta_v^*\|_{L^2(\partial\Omega_j)} + \|\tilde{e}_v\|_{L^2(\partial\Omega_j)}\|\delta_{\mathbf{w}}^*\cdot\mathbf{n}\|_{L^2(\partial\Omega_j)}\\ &\leq C\sqrt{\mathcal{E}^h}\left(h^{\bar{q}}\left(|u(\cdot,t)|_{H^{\bar{q}+2}(\Omega)} + |v(\cdot,t)|_{H^{\bar{q}+1}(\Omega)}\right) + h^{q+1}\left|\frac{\partial v}{\partial t}(\cdot,t)\right|_{H^{q+1}(\Omega)}\right).\end{aligned}$$

Then a direct integration in time combined with the assumption that $(\tilde{e}_u, \tilde{e}_v) = 0$ at $t = 0$ yields

$$\mathcal{E}^h(T) \leq CT\max_{t\leq T}\left(h^{2\bar{q}}\left(|u(\cdot,t)|^2_{H^{\bar{q}+2}(\Omega)} + |v(\cdot,t)|^2_{H^{\bar{q}+1}(\Omega)}\right) + h^{2q+2}\left|\frac{\partial v}{\partial t}(\cdot,t)\right|^2_{H^{q+1}(\Omega)}\right). \tag{3.21}$$

Since $e_v = \tilde{e}_v - \delta_v$, $e_u = \tilde{e}_u - \delta_u$, (3.15) follows from the triangle inequality and an invocation of (3.17).

For dissipative fluxes, $\tau, \beta, \gamma > 0$, we can improve the estimate. For internal boundaries we have using (3.11) and the last line in (3.13) that the contribution is

$$\begin{aligned}-c^2\sum_k\int_{F_k}[[\nabla\tilde{e}_u]]\delta_v^* + [[\tilde{e}_v]]\cdot\delta_{\mathbf{w}}^* - \sum_k\int_{F_k}\tau\,|[[\tilde{e}_v]]|^2 + \tau c^2[[\nabla\tilde{e}_u]]^2 &\leq C\sum_k\left(\|\delta_v^*\|^2_{L^2(F_k)} + \|\delta_{\mathbf{w}}^*\|^2_{L^2(F_k)}\right)\\ &\leq Ch^{2\bar{q}+1}\left(|u(\cdot,t)|^2_{H^{\bar{q}+2}(\Omega)} + |v(\cdot,t)|^2_{H^{\bar{q}+1}(\Omega)}\right).\end{aligned} \tag{3.22}$$

On the physical boundary we obtain:

$$-c^2\sum_k\int_{B_k}\left(\nabla\tilde{e}_u\cdot\mathbf{n}\right)\delta_v^* + \tilde{e}_v\delta_{\mathbf{w}}^*\cdot\mathbf{n} - \gamma\left(a\tilde{e}_v + bc\nabla\tilde{e}_u\cdot\mathbf{n}\right)^2 - ab\left(\tilde{e}_v^2 + c^2\left(\nabla\tilde{e}_u\cdot\mathbf{n}\right)^2\right). \tag{3.23}$$

In the case where both $a > 0$, $b > 0$ we can proceed as in the derivation of (3.22) to obtain a contribution bounded by

$$C\sum_k\left(\|\delta_v^*\|^2_{L^2(B_k)} + \|\delta_{\mathbf{w}}^*\|^2_{L^2(B_k)}\right) \leq Ch^{2\bar{q}+1}\left(|u(\cdot,t)|^2_{H^{\bar{q}+2}(\Omega)} + |v(\cdot,t)|^2_{H^{\bar{q}+1}(\Omega)}\right). \tag{3.24}$$

Suppose $a = 1$, $b = 0$. Then by (2.25), (2.33) $\delta_v^* = 0$ so that the boundary contribution satisfies

$$-\sum_k\int_{B_k}c^2\tilde{e}_v\delta_{\mathbf{w}}^*\cdot\mathbf{n} + \gamma\left(\tilde{e}_v\right)^2 \leq C\sum_k\|\delta_{\mathbf{w}}^*\|^2_{L^2(B_k)} \leq Ch^{2\bar{q}+1}\left(|u(\cdot,t)|^2_{H^{\bar{q}+2}(\Omega)} + |v(\cdot,t)|^2_{H^{\bar{q}+1}(\Omega)}\right). \tag{3.25}$$

Similarly if $a = 0$, $b = 1$ then $\delta_{\mathbf{w}}^*\cdot\mathbf{n} = 0$ and we obtain

$$-c^2\sum_k\int_{B_k}\left(\nabla\tilde{e}_u\cdot\mathbf{n}\right)\delta_v^* + \gamma\left(\nabla\tilde{e}_u\cdot\mathbf{n}\right)^2 \leq C\sum_k\|\delta_v^*\|^2_{L^2(B_k)} \leq Ch^{2\bar{q}+1}\left(|u(\cdot,t)|^2_{H^{\bar{q}+2}(\Omega)} + |v(\cdot,t)|^2_{H^{\bar{q}+1}(\Omega)}\right). \tag{3.26}$$

Combining (3.22) with any of (3.24)-(3.26) yields

$$\frac{d\mathcal{E}^h}{dt} \leq C\sqrt{\mathcal{E}^h}\left(h^{\bar{q}+1/2}\left(|u(\cdot,t)|_{H^{\bar{q}+2}(\Omega)} + |v(\cdot,t)|_{H^{\bar{q}+1}(\Omega)}\right) + h^{q+1}\left|\frac{\partial v}{\partial t}(\cdot,t)\right|_{H^{q+1}(\Omega)}\right). \tag{3.27}$$

Then again (3.15) with $\sigma = \frac{2\bar{q}+1}{2}$ follows by direct integration in time combined with (3.17). This completes the proof.$\diamond$

REMARK 1. *We note that the formula for $\bar{q}$ indicates that a given accuracy can be achieved using the fewest degrees of freedom if $s = q+1$, which we typically use in the experiments. The requirements for proving optimal error estimates stated below are more restrictive as the proof only works when $s = q+1$. Some experiments with $s = q$ are presented. For the central flux increasing q sometimes led to an improvement in the convergence rate for u, but in general the approximation to v was not improved, and in the case of the alternating flux it was degraded.*

3.2. Improved estimates for $d = 1$. We now assume that $s = q+1$, as discussed in Remark 1. As required in the analysis of upwind DG methods for first order systems (e.g. [12]), we now seek to define $(\tilde{u}^h, \tilde{v}^h)$ so that the boundary terms in $\mathcal{B}(\tilde{D}_0^h, \Delta^h)$ vanish; that is

$$\delta_v^* = \delta_{\mathbf{w}}^* \cdot \mathbf{n} = 0.$$

For our general flux form, an analysis of the underlying algebraic system shows that this can be accomplished under the condition

$$\alpha(1-\alpha) = \beta\tau, \tag{3.28}$$

assuming a consistent choice of α; for example the element labelled 1 always lying to the left of the element labelled 2, which will now be our convention. Clearly (3.28) is satisfied for the alternating and Sommerfeld fluxes but not for the central flux. Precisely, imposing (3.28) we can transform (3.2) into independent equations involving only variables from one element. Then we can satisfy (3.2) by imposing the boundary conditions on the endpoints of the element $\Omega_j = (x_{j-1}, x_j)$:

$$(1+\beta-\alpha)\delta_v + (\tau+\alpha)c\frac{\partial \delta_u}{\delta x} = 0, \quad x = x_{j-1}, \tag{3.29}$$

$$(\beta+\alpha)\delta_v - (1+\tau-\alpha)c\frac{\partial \delta_u}{\delta x} = 0, \quad x = x_j. \tag{3.30}$$

We then construct δ_v and δ_u by requiring the following:
i For all $\phi \in \Pi^{q-1}$

$$\int_{x_{j-1}}^{x_j} c^2\phi\frac{d\delta_u}{dx} = \int_{x_{j-1}}^{x_j} c^2\phi\delta_v = 0, \tag{3.31}$$

ii Zero average error of u

$$\int_{x_{j-1}}^{x_j} \delta_u = 0, \tag{3.32}$$

iii Equations (3.29)-(3.30) hold.

We then have:

LEMMA 3.1. *The function $(\tilde{u}^h, \tilde{v}^h)$ is uniquely defined by (3.29)-(3.32) for $(u,v) \in H^{q+3}(\Omega) \times H^{q+2}(\Omega)$ and there exists a constant C such that for $h = \max|x_j - x_{j-1}|$*

$$\|\frac{\partial \delta_u}{\partial t}\|_{H^1(\Omega)} + \|\frac{\partial \delta_v}{\partial t}\|_{L^2(\Omega)} \leq Ch^{q+1}\left(|v|_{H^{q+2}(\Omega)} + \left|\frac{\partial v}{\partial t}\right|_{H^{q+1}(\Omega)}\right). \tag{3.33}$$

Proof: The dimensionality of the local polynomial space $\Pi^{q+1} \times \Pi^q$ is $2q+3$ which matches the number of linear equations. Suppose $u = v = 0$. Then on Ω_j conditions (3.31) imply that $\tilde{v}^h$ and $\frac{d\tilde{u}^h}{dx}$ are degree-q polynomials orthogonal in the c^2-weighted inner product to all polynomials of lower degree. As such any nonzero linear combination must have all q zeros in the interior of the interval. Hence using the boundary conditions it is obvious that $\tilde{v}^h = \frac{d\tilde{u}^h}{dx} = 0$ on Ω_j. A subsequent use of condition (3.32) implies $\tilde{u}^h = 0$. Thus $(\tilde{u}^h, \tilde{v}^h)$ is

uniquely defined and preserves the space $\Pi^{q+1} \times \Pi^q$. To derive the error estimates we note that the polynomial approximation system commutes with time differentiation. Using the Bramble-Hilbert lemma and replacing $\frac{\partial u}{\partial t}$ by v the result follows.$\diamond$

We can now prove an optimal error estimate for the energy:

THEOREM 4. *Suppose $d = 1$, $s = q + 1$, and the solution satisfies $U(\cdot, t) \in H^{q+2}(\Omega) \times H^{q+1}(\Omega)$. Suppose further that the initial condition for the DG solution satisfies error estimates commensurate with Lemma 3.1. Then there exists C independent of U and h such that for any $T > 0$*

$$\|e_v(\cdot, T)\|^2_{L^2(\Omega)} + \|\nabla e_u(\cdot, T)\|^2_{L^2(\Omega)} \leq C(1+T)h^{2q+2} \max_{t \leq T} \left(|v|^2_{H^{q+2}(\Omega)} + \left| \frac{\partial v}{\partial t} \right|^2_{H^{q+1}(\Omega)} \right). \tag{3.34}$$

Proof: Repeating the proof of Theorem 3 using $(\tilde{u}^h, \tilde{v}^h)$ defined by (3.31)-(3.30) we obtain in place of (3.13)

$$\begin{aligned}
\mathcal{B}(\tilde{D}^h_0, \Delta^h) &= \sum_j \int_{x_{j-1}}^{x_j} c^2 \frac{\partial \tilde{e}_u}{\partial x} \cdot \frac{\partial}{\partial x} \left(\frac{\partial \delta_u}{\partial t} - \delta_v \right) + \tilde{e}_v \frac{\partial \delta_v}{\partial t} + c^2 \frac{\partial \tilde{e}_v}{\partial x} \cdot \frac{\partial \delta_u}{\partial x} \\
&\quad + \sum_j c^2 \frac{\partial \tilde{e}_u}{\partial x} (\delta_v - \delta^*_v) - \tilde{e}_v \delta^*_{\mathbf{w}} |^{x_j}_{x_{j-1}} \\
&= \sum_j \int_{x_{j-1}}^{x_j} c^2 \frac{\partial^2 \tilde{e}_u}{\partial x^2} \delta_v + 2cc' \frac{\partial \tilde{e}_u}{\partial x} \cdot \frac{\partial \delta_u}{\partial t} + \tilde{e}_v \frac{\partial \delta_v}{\partial t} \\
&= \sum_j \int_{x_{j-1}}^{x_j} 2cc' \frac{\partial \tilde{e}_u}{\partial x} \cdot \frac{\partial \delta_u}{\partial t} + \tilde{e}_v \frac{\partial \delta_v}{\partial t}. \qquad (3.35)
\end{aligned}$$

Combining (3.35), the estimates of Lemma 3.1, and the non-positivity of the boundary contributions we obtain

$$\frac{d\mathcal{E}^h}{dt} \leq Ch^{q+1} \sqrt{\mathcal{E}^h} \left(|u(\cdot, t)|^2_{H^{q+3}(\Omega)} + |v(\cdot, t)|^2_{H^{q+2}(\Omega)} \right)^{1/2}. \tag{3.36}$$

Integrating yields the final result.$\diamond$

REMARK 2. *Estimates for $d = 1$ as proven above can typically be generalized to Cartesian grids (e.g. [12]), but we will not pursue this generalization here. In the numerical experiments below we observe optimal convergence in the energy norm for both the upwind and alternating flux even for non-Cartesian grids built from quadrilateral elements. For the central flux, on the other hand, convergence is suboptimal even on Cartesian grids for odd q and, for even q, is degraded in the non-Cartesian case.*

REMARK 3. *The numerical experiments also show L^2-convergence at one order higher than convergence for the energy. However, the typical method to prove this in the Galerkin setting, apparently originating in the work of Baker [3], does not seem to be directly applicable to our formulation. Establishing this superconvergence rigorously is a topic for future study.*

4. Discretization and Numerical Examples. In this section we describe the implementation of our method and present experiments to determine the convergence rate in both the energy and L^2 norms, as well as study the effect of the flux choice on the spectral radius of the spatial operators.

As the order of the approximation is one degree higher for the displacement than for the velocity in most of our experiments, it is slightly more convenient to work with a modal formulation than a nodal formulation, although a nodal formulation is certainly possible too. For simplicity we take $f = 0$ and, except when considering variable coefficients, set $c = 1$. We have carried out additional experiments with $f \neq 0$ and verified that the same convergence behavior holds.

4.1. Modal formulation. Starting with $d = 1$, assume that the computational domain has been discretized by a uniform grid $x_0, \ldots, x_j, x_{j+1}, \ldots x_n$ with spacing h. Let $x_{j+\frac{1}{2}} = (x_j + x_{j+1})/2$ then the mapping $z = \frac{2}{h}(x - x_{j+\frac{1}{2}})$ takes element Ω_j to the reference element $\Omega_{\mathrm{R}} = [-1, 1]$ where we expand the displacement and

velocity in test functions:

$$u_j^h(x,t) = \sum_{l=0}^{q+1} \hat{u}_{l,j}^h(t)\phi_l(z), \tag{4.1}$$

$$v_j^h(x,t) = \sum_{l=0}^{q} \hat{v}_{l,j}^h(t)\psi_l(z). \tag{4.2}$$

It is convenient to arrange the expansion coefficients into $\hat{\mathbf{u}} = [\hat{u}_{0,j}^h, \hat{u}_{1,j}^h, \ldots, \hat{u}_{q+1,j}^h]^T$ and $\hat{\mathbf{v}} = [\hat{v}_{0,j}^h, \hat{v}_{1,j}^h, \ldots, \hat{v}_{q,j}^h]^T$. The discrete version of (2.11) on an element can then be written

$$M^v \hat{\mathbf{v}}'(t) + S^u \hat{\mathbf{u}}(t) = \mathcal{F}^v. \tag{4.3}$$

The extra equation (2.14) and the variational equation (2.10) can also be assembled into the system

$$M^u \hat{\mathbf{u}}'(t) + S^v \hat{\mathbf{v}}(t) = \mathcal{F}^u, \tag{4.4}$$

where the exact expressions for the mass and stiffness matrices and the flux terms can be found in Appendix A.

Here we use Chebyshev polynomials as the test and trial functions:

$$\psi_l(z) = \phi_l(z) = T_l(z) = \cos(lt), \quad t = \arccos(z). \tag{4.5}$$

To compute integrals required for the least squares expansion of the initial data and the matrix coefficients in the variable coefficient case, we use sufficiently high order Chebyshev quadrature.

REMARK 4. *We have also carried out experiments with the Chebyshev basis replaced by the Legendre basis and the monomial basis. Results with the Legendre basis were essentially the same as those reported here, while not unexpectedly considering the loss of conditioning with increasing degree, some degradation of convergence was observed for high-order methods constructed with the monomial basis.*

Our two dimensional solver is formulated on quadrilaterals and the expansions of the displacement and velocity are performed on the reference element using tensor product Chebyshev polynomials. The classic fourth order accurate Runge-Kutta method (RK4) is used to discretize in time.

4.2. Verification of order of accuracy for $d = 1$. To investigate the order of accuracy of the methods we solve $u_{tt} = u_{xx}$ on $-1 \leq x \leq 1, t > 0$ with periodic boundary conditions and with initial data chosen such that the solution is the traveling wave $\sin(\pi(x-t))$. The discretization is performed on a uniform grid $x_i = ih$, $i = 0, n$, $h = 2/n$. The time step is chosen as $\Delta t = h^2/20$ so that the error is dominated by the spatial error. We report the l_2-error in the displacement u^h and in the velocity v^h.

Four different fluxes are considered, the Sommerfeld flux with $\zeta = 1$ (denoted S.-flux), the alternating flux (denoted A.-flux), the centered flux (denoted C.-flux) and finally the alternating flux with the same jump penalization (same τ and β) as for the Sommerfeld flux (denoted A.+U.-flux.) We also consider two choices for the degrees of the approximation spaces; either we take the degree of v^h to be one less than u^h or we take them to be the same.

The errors for u^h plotted against the grid-spacing for the different fluxes and different orders of approximation are displayed in Figure 4.1. The results for v_h are displayed in 4.2. Linear least squares estimates of the rates of convergence from the error curves in the figures can be found in Table 4.1 and 4.2 for different and same order of approximation.

The convergence rates for u^h behave much as expected. When u^h is approximated by a degree 3 or higher polynomial we see optimal convergence for the A., S. and A.+S.-fluxes independent of the degree of v^h. For the central flux with u^h and v^h having different degree we see suboptimal convergence in u^h for the central flux while for u^h and v^h being the same degree the convergence rate for u^h appears to be close to optimal. For very very low orders (u^h being degree 1 and 2) we see slightly suboptimal convergence rates for all fluxes and for both combinations of approximation spaces. Generally the error levels and convergence rates for the alternating and dissipative fluxes are comparable, but the behavior of the dissipative methods is more predictable.

The empirically determined convergence for v^h differs between the cases when u^h and v^h are of the same and different degree. When the degree is different we observe convergence rates coinciding with the degree of v^h

TABLE 4.1
Estimated rates of convergence for $d = 1$ and one degree lower approximation for v.

Degree of approx. of u	1	2	3	4	5	6	7
Rate from LS fit S.-flux u	1.5127	2.2520	4.1333	4.9752	6.0953	6.8919	7.9622
Rate from LS fit S.-flux v	0.9922	1.9338	3.0027	3.9742	5.0066	6.0325	7.0034
Rate from LS fit A.-flux u	1.5257	2.3265	4.2062	4.8286	6.1042	6.9366	8.0046
Rate from LS fit A.-flux v	0.9828	2.1072	3.1364	4.0891	5.0667	6.0471	7.0053
Rate from LS fit C.-flux u	2.0737	1.9893	4.2856	4.0941	6.1006	5.9141	8.0911
Rate from LS fit C.-flux v	1.0067	1.0158	3.1772	2.8793	5.0999	4.9418	7.1152
Rate from LS fit A+U-flux u	1.9284	2.2083	4.3960	4.8773	6.1752	6.8458	8.0492
Rate from LS fit A+U-flux v	1.0052	2.0152	2.9577	4.0728	4.9849	6.0793	6.9356

TABLE 4.2
Estimated rates of convergence for $d = 1$. Here u and v are in the same space.

Degree of approx. of u	1	2	3	4	5	6	7
Rate from LS fit S.-flux u	1.9812	2.8098	4.2334	5.2025	6.1273	6.9178	7.9241
Rate from LS fit S.-flux v	1.6067	1.8788	3.0452	3.9528	5.0137	6.0516	7.0117
Rate from LS fit A.-flux u	1.1203	2.5590	4.1036	5.2299	6.1033	6.9413	7.9277
Rate from LS fit A.-flux v	-0.0654	1.0148	2.0081	3.0165	3.9943	4.9842	5.9861
Rate from LS fit C.-flux u	1.9859	2.2203	4.5079	5.3373	6.2078	6.9131	8.1310
Rate from LS fit C.-flux v	0.9184	1.0019	2.9883	2.9650	4.9424	4.9536	7.0190
Rate from LS fit A+U-flux u	1.8540	2.8402	4.3109	5.2262	6.1809	6.9379	7.9564
Rate from LS fit A+U-flux v	0.8102	1.7296	2.7742	3.9422	4.9024	6.0287	6.9332

for all fluxes, but when the degree is the same we observe degradation of two orders in the rate of convergence (compared to the rate for u^h) when the alternating flux is used. In the most severe case, when u^h and v^h are linear, this results in loss of convergence for v^h. We note that this result is in agreement with the sharp (in the worst sense) application of Theorem 3.

Looking at the actual error curves in Figures 4.1 and 4.2 we find that the errors in u^h are for the most part comparable for the two choices of approximation spaces and fluxes. For the errors in v^h we see that using different degree approximation spaces give similar or better results for all fluxes except for the Sommerfeld flux where the results are slightly better for the same degree.

4.3. A Variable Coefficient Example. As an example with a variable coefficient we solve $u_{tt} = (c^2(x)u_x)_x$ with $c^2(x) = 1 + \sin(\pi x)/10$ on $-1 \le x \le 1, t > 0$ with periodic boundary conditions and with initial data $u = \sin(\pi x), v = -\pi\cos(\pi x)$. The discretization is performed on a uniform grid $x_i = -1 + ih$, $i = 0, n$, $h = 2/n$ and with $s = q + 1$. The time step is chosen as $\Delta t = 0.05h/(q+1)^2$ and we solve until time 0.1. In Table 4.3 we list the rates of convergence for the displacement u^h for $q + 1 = 3, \ldots, 8$. The error is computed against a reference solution obtained with $q + 1 = 10$. The results are generally comparable to those obtained in the constant coefficient case.

4.4. Spectrum and spectral radii. To predict the timestep restrictions we compute the eigenvalues, λ, of the time stepping operator,

$$\lambda M^v \hat{\mathbf{v}} + S^u \hat{\mathbf{u}} = 0, \quad \lambda M^u \hat{\mathbf{u}} + S^v \hat{\mathbf{v}} = 0, \tag{4.6}$$

for the three different fluxes on a sufficiently fine grid. We also empirically determine the largest possible stable ratio $\Delta t/h$ and plot its scaled inverse (we scale by $\sqrt{8}$ as we use RK4). The empirically computed data agrees well with the predictions based on the spectral radii.

As the alternating flux and the central flux are both energy conserving their spectra are confined to the imaginary axis and we only report the spectral radii; see the left part of Figure 4.4. For the Sommerfeld flux we also report the full spectrum, see the right part of Figure 4.4.

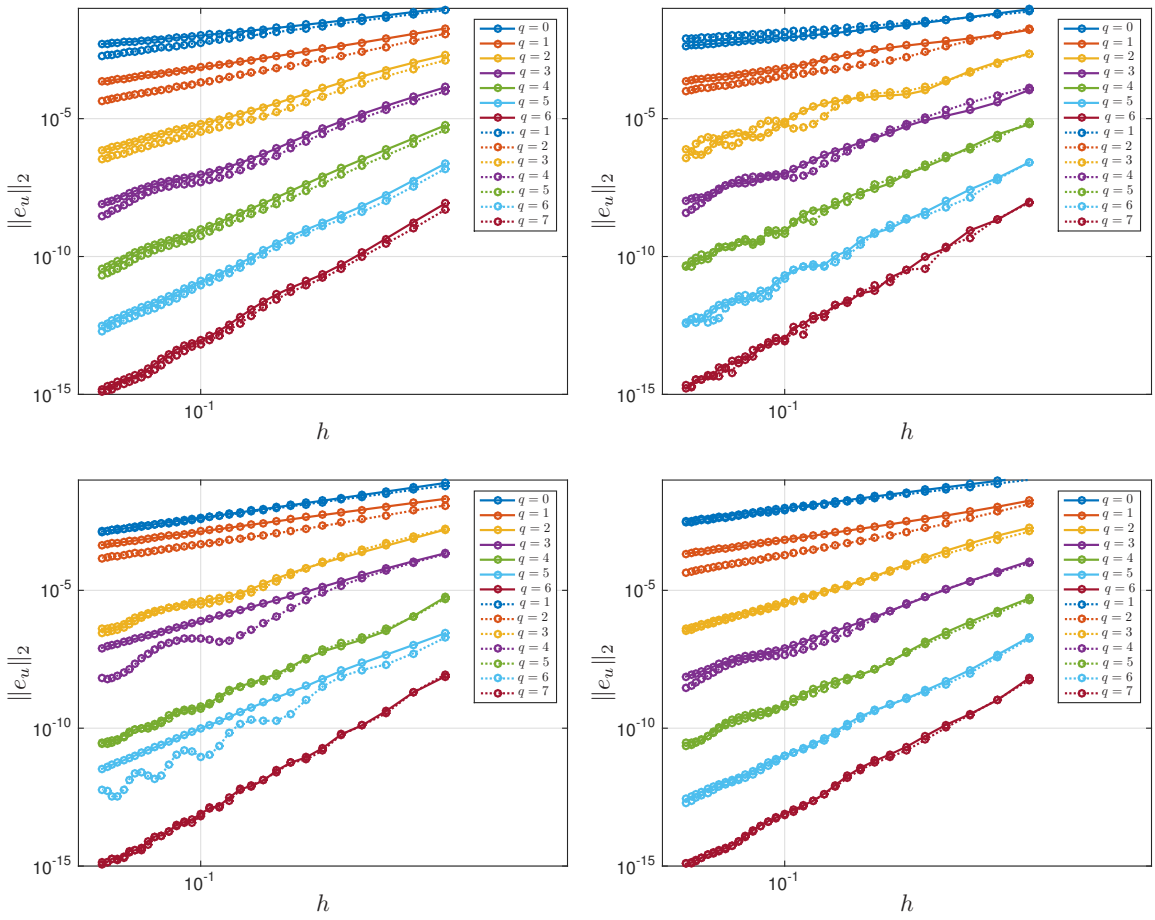

FIG. 4.1. *Plots of the error in u as a function of h in $d = 1$: on the top, from left to right, Sommerfeld and alternating, on the bottom, from left to right, central and alternating with upwind dissipation. In the legend q is the degree of the approximation of v. The solid lines are for results when u and v are in different spaces, the dotted are when they are in the same space.*

TABLE 4.3
Rates of convergence obtained from a linear least squares fit to the data in Figure 4.3.

$q+1$	3	4	5	6	7	8
Rate from LS fit S.-flux	4.43	5.66	6.20	6.82	7.93	9.00
Rate from LS fit C.-flux	4.62	4.18	6.28	5.78	8.68	8.06
Rate from LS fit A.-flux	4.57	5.41	6.18	7.07	7.85	9.00

4.5. Empirical order of accuracy for $d = 2$. In two dimensions we solve $u_{tt} = u_{xx} + u_{yy}$ on $(x, y) \in [-\pi, \pi]^2$ with periodic boundary conditions and initial data chosen so that $u(x, y, t) = \sin(x + y + \sqrt{2}t)$. We consider regular Cartesian grids with elements whose sides are $h_x = h_y = 2\pi/n$, as well as unstructured grids. The unstructured grids are obtained by perturbing the x and y coordinates of the interior nodes of the Cartesian grid by a uniformly distributed random perturbation $(\Delta x, \Delta_y)$ taking values in $[-h_x/10, h_x/10]\times[-h_y/10, h_y/10]$.

We evolve the solution until $T = 0.2$ with CFL $= (0.1, 0.05, 0.01, 0.005)$ for $q =$ (0-1, 2-4, 5, 6). The l_2 and energy norms of the errors as a function of $h_x = h_y$ for $q = 0, \ldots, 6$ can be found in Figures 4.5 and 4.6 for the regular and perturbed grid respectively. Least squares fits for the rates of convergence can be found in Tables 4.4 and 4.5.

For the regular grid we observe the same results as in the one-dimensional case, the Sommerfeld and alternating fluxes yield optimal convergence rates $q + 2$ (the exception is $q = 1$ where the convergence rate appears

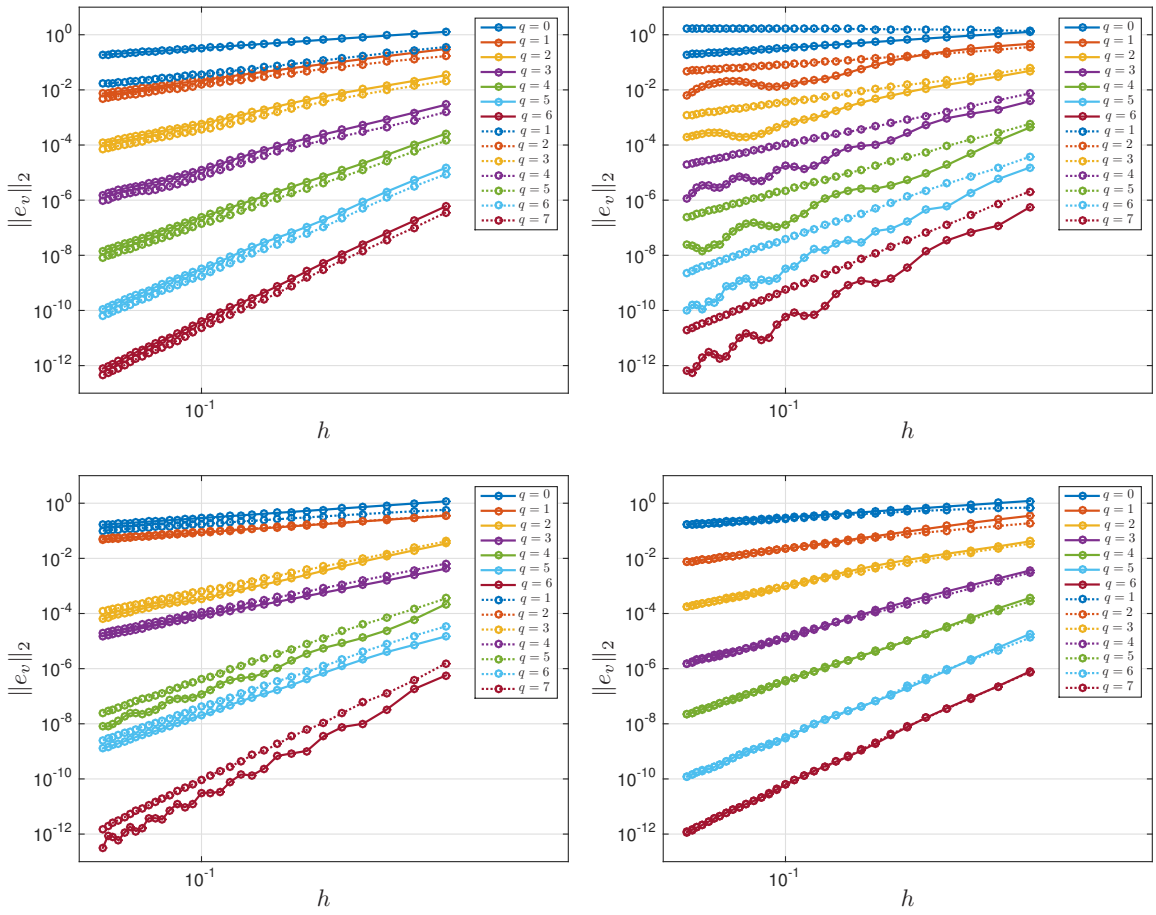

FIG. 4.2. *Plots of the error in v as a function of h in $d = 1$: on the top, from left to right, Sommerfeld and alternating, on the bottom, from left to right, central and alternating with upwind dissipation. In the legend q is the degree of the approximation of v. The solid lines are for results when u and v are in different spaces, the dotted are when they are in the same space.*

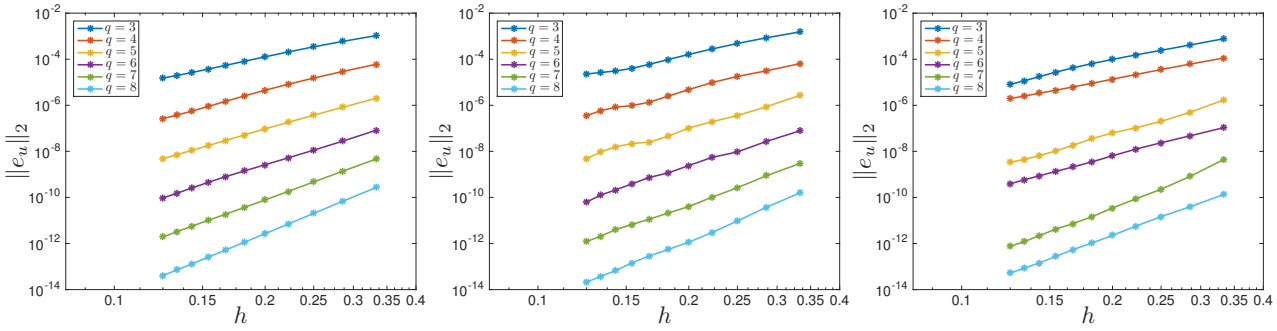

FIG. 4.3. *Errors for the variable coefficient example. From left to right Sommerfeld, alternating and central fluxes.*

to be q possibly due to the error not being in the asymptotic regime) while for the central flux the convergence rates are sub-optimal and increase in steps of two as above. For the randomly perturbed grid the rates remain the same for the Sommerfeld and alternating fluxes but appear to deteriorate by roughly half an order for $q+1$ odd when the central flux is employed.

4.6. Conservation of energy. Finally we perform an experiment to assess the energy conservation and dissipation properties of our method when using the conservative and dissipative fluxes. We consider an example

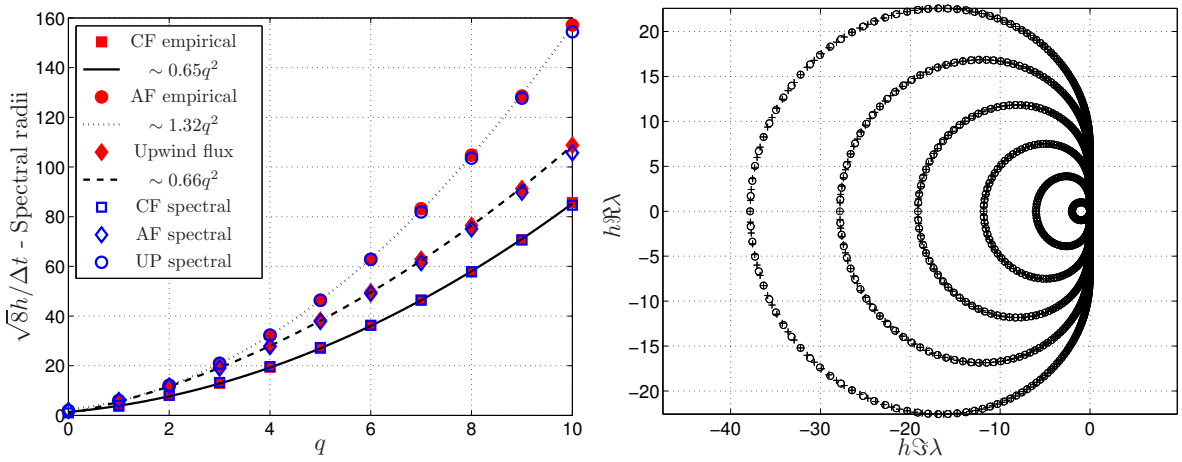

FIG. 4.4. *To the left: empirically determined CFL number (in red) and spectral radii (scaled by h) of the time stepping operator (in blue) as a function of q for the three different fluxes. Also plotted is the least squares fit of a quadratic to the empirically determined data. To the right the full spectrum for the Sommerfeld flux is shown for $q = 0, \ldots, 5$ (also scaled by h).*

TABLE 4.4
Rates of convergence for regular Cartesian grids and $d = 2$.

Degree $q+1$ for approx. of u	1	2	3	4	5	6	7
Rate for u from LS fit S.-flux	1.384	2.127	4.003	5.052	6.112	6.974	7.889
Rate for E from LS fit S.-flux	0.847	1.714	2.921	3.961	5.020	6.109	7.052
Rate for u from LS fit A.-flux	1.5727	2.003	3.525	4.740	5.772	6.787	7.839
Rate for E from LS fit A.-flux	0.8944	1.829	2.779	4.130	5.041	6.035	6.874
Rate for u from LS fit C.-flux	2.127	1.904	4.318	3.925	6.193	6.025	7.750
Rate for E from LS fit C.-flux	1.099	0.890	3.650	2.985	5.445	4.911	7.342

on the domain $(x, y) \in [-6, 6]^2$ with periodic boundary conditions in the y-direction and homogeneous Dirichlet and Neumann boundary conditions to the left and right respectively. The initial data is chosen to be

$$u(x, y, 0) = e^{-(x^2+y^2)}, \quad v(x, y, 0) = 0,$$

and we evolve the data until time $T = 25$.

The size of the domain ensures that the initial data is close to zero at the boundary and the energy is thus very close to the energy $E(0) = E(t) \equiv \pi$ for the unbounded problem.

The computational domain is discretized by 10×10 elements with the interior nodes perturbed as described above. The CFL number is fixed at 0.005 for all orders. In Figure 4.7 results using $q = 1, \ldots, 6$ and with central or upwind flux are shown. To the left we compare the discrete energy to its initial value. We find that when a central flux or alternating flux is used the decay is very small, on the order of 10^{-10}. For the Sommerfeld flux the decay is in general larger but becomes smaller as the order of approximation is increased. To the right in Figure 4.7 we plot the error in the discrete energy measured against the exact energy. Here the error when using the central flux or alternating flux are practically flat while the error obtained using the Sommerfeld flux shows some variations with time. The level of the error appears to decrease in a similar fashion for both fluxes as the order of approximation increases.

5. Extensions. This paper has focused on the construction of the method for linear problems and its application to the scalar wave equation. However, our general formulation can be applied much more broadly. In a forthcoming paper [2] we apply the general formulation to the elastic wave equation. If the elastic material properties jump (this is the case for most problems in seismology) it can be somewhat involved to determine numerical fluxes that satisfy the interface conditions (continuity of traction and displacement) at element interfaces, see e.g. [17]. In [2] we find that the general formulation presented here can be applied directly and without

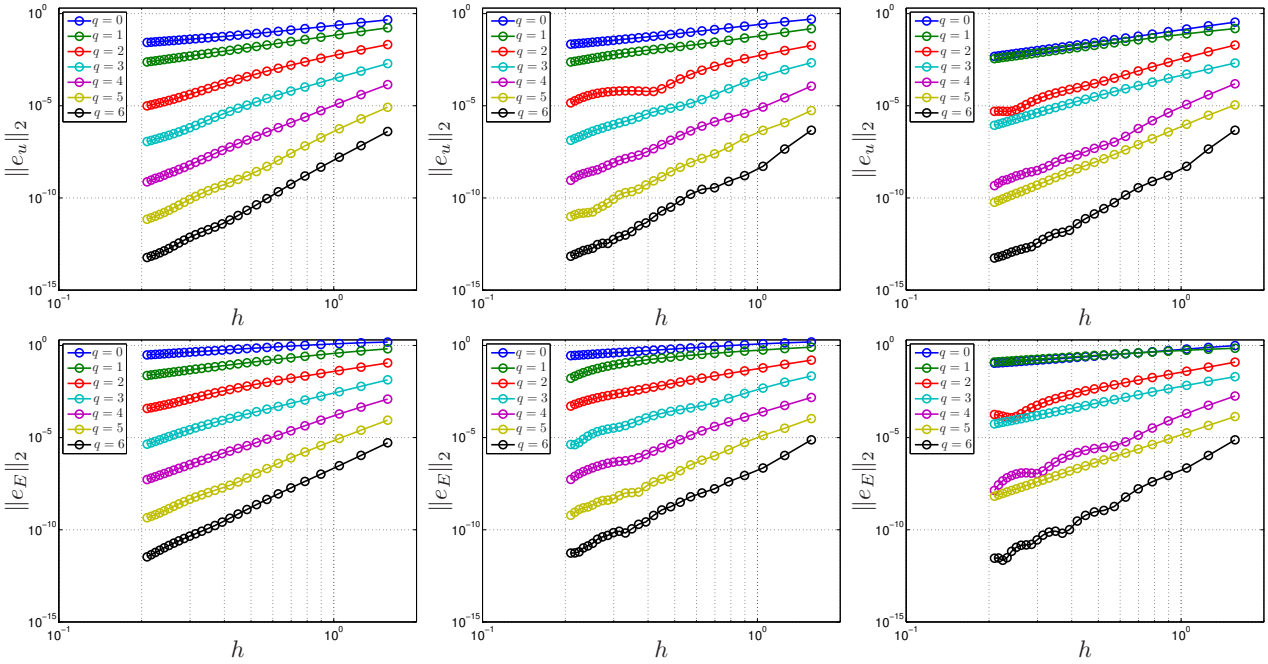

FIG. 4.5. *Convergence in 2D for regular grids. From left to right Sommerfeld, alternating and central fluxes.*

TABLE 4.5
Rates of convergence for the randomly perturbed grids in 2D.

Degree $q+1$ for approx. of u	1	2	3	4	5	6	7
Rate for u from LS fit S.-flux	1.353	2.123	3.873	5.010	6.078	6.963	7.902
Rate for E from LS fit S.-flux	0.769	1.687	2.867	3.925	4.975	6.045	6.988
Rate for u from LS fit A.-flux	1.399	1.998	3.504	4.723	5.738	6.775	7.803
Rate for E from LS fit A.-flux	0.664	1.773	2.746	4.047	4.984	5.974	6.995
Rate for u from LS fit C.-flux	1.437	1.898	3.441	3.938	5.543	6.044	7.321
Rate for E from LS fit C.-flux	0.618	0.891	2.644	2.996	4.506	4.939	6.340

modification of the numerical flux specification to such problems. The resulting method automatically satisfies the interface conditions.

For nonlinear problems we have carried out numerical experiments for the sine-Gordon equation as well as for wave equations where the speed depends nonlinearly on the solution. In the first case the nonlinearity can simply be treated as a forcing term whose contribution can be incorporated by evaluating the nonlinearity in a pseudo-spectral manner at the quadrature points. For the second problem with a nonlinear wave speed the mass and stiffness matrices depend on the solution and have to be recomputed (again in a pseudo-spectral manner) at each timestep. In our simulations of these nonlinear systems we so far observe the same convergence and conservation properties as in the linear case but we plan to carry out a more rigorous analysis and more

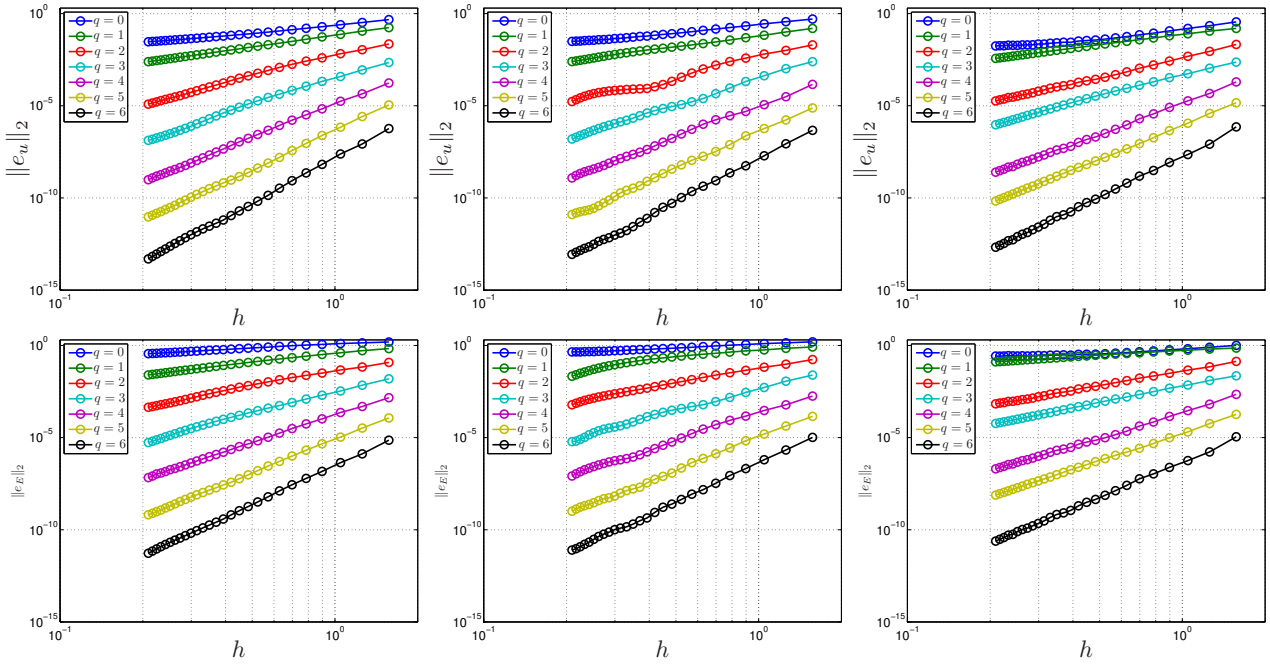

FIG. 4.6. *Convergence in 2D for randomly perturbed grids. From left to right Sommerfeld, alternating and central fluxes*

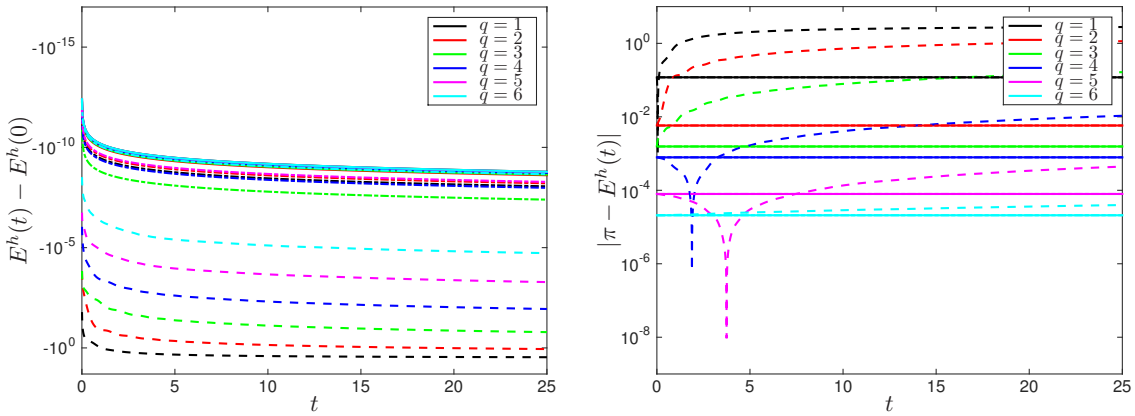

FIG. 4.7. *To the left: decay of the discrete energy from its initial value. To the right: the error in the discrete energy. Dashed lines are results with the Sommerfeld flux and solid lines are results with the central flux, dash dotted is the alternating flux.*

extensive numerical experiments to confirm our preliminary, but promising, results.

Appendix A. Flux terms, mass and stiffness matrices . The mass and stiffness matrices are:

$$M^v_{k,l} = \frac{h}{2}\int_{-1}^{1} \psi_k(z)\,\psi_l(z)dz, \qquad k,l = 0,\dots,q, \tag{A.1}$$

$$M^u_{0,l} = \frac{h}{2}\int_{-1}^{1} \phi_l(z)dz, \qquad l = 0,\dots,s, \tag{A.2}$$

$$M^u_{k,l} = \frac{h}{2}\frac{4}{h^2}\int_{-1}^{1} \phi_k''(z)\,\phi_l(z)dz - \left[\frac{2}{h}\phi_k'(z)\,\phi_l(z)\right]_{-1}^{1}, \qquad k = 1,\dots,s, \quad l = 0,\dots,s, \tag{A.3}$$

$$S^v_{0,l} = -\frac{h}{2}\int_{-1}^{1} \psi_l(z)dz, \qquad l = 0,\dots,q, \tag{A.4}$$

$$S^v_{k,l} = -\frac{h}{2}\frac{4}{h^2}\int_{-1}^{1} \psi_k''(z)\,\phi_l(z)dz, \qquad k = 1,\dots,s,\ l = 0,\dots,q, \tag{A.5}$$

$$S^u_{k,l} = \frac{h}{2}\frac{4}{h^2}\int_{-1}^{1} \psi_k'(z)\,\phi_l'(z)dz, \qquad k = 0,\dots,q, \quad l = 0,\dots,s. \tag{A.6}$$

Here the factors $\frac{h}{2}$, $\frac{2}{h}$ appear from the integral and derivative due to the change of variables. The flux terms are

$$\mathcal{F}_l^v = \left[\left(\frac{\partial u}{\partial x} \right)^* \psi_l(z(x)) \right]_{x_j}^{x_{j+1}}, \quad l = 0, \ldots, q, \tag{A.7}$$

$$\mathcal{F}_l^u = -\frac{2}{h} \left[v^* (\nabla_z \phi_l(z(x)) \cdot n) \right]_{x_j}^{x_{j+1}}, \quad l = 0, \ldots, s. \tag{A.8}$$

For the numerical experiments presented in this paper we compute the integrals exactly by using sufficiently high order Gauss quadrature.

REFERENCES

[1] C. Agut, J.-M. Bart, and J. Diaz, *Numerical study of the stability of the interior penalty discontinuous Galerkin method for the wave equation with 2D triangulations*, Tech. Report 7719, INRIA, 2011.

[2] D. Appelö and T. Hagstrom, *An energy-based discontinuous Galerkin discretization of the elastic wave equation in second order form*. In preparation, 2015.

[3] G. Baker, *Error estimates for finite element methods for second order hyperbolic equations*, SIAM J. Num. Anal., 13 (1976), pp. 564–576.

[4] X. Chen, D. Appelö, and T. Hagstrom, *A hybrid Hermite - discontinuous Galerkin method for hyperbolic systems with application to Maxwell's equations*, J. Comput. Phys., 257 (2014), pp. 501–520.

[5] C.-S. Chou, C.-W. Shu, and Y. Xing, *Optimal energy conserving local discontinuous Galerkin methods for second-order wave equation in heterogeneous media*, Journal of Computational Physics, 272 (2014), pp. 88–107.

[6] E. Chung and B. Engquist, *Optimal discontinuous Galerkin methods for wave propagation*, SIAM J. Num. Anal., 44 (2006), pp. 2131–2158.

[7] ———, *Optimal discontinuous Galerkin methods for the acoustic wave equation in higher dimensions*, SIAM J. Num. Anal., 47 (2009), pp. 3820–3848.

[8] P. Ciarlet, *The finite element method for elliptic problems*, Classics in Applied Mathematics 40, SIAM, Philadelphia, 2002.

[9] M. Grote, A. Schneebeli, and D. Schötzau, *Discontinuous Galerkin finite element method for the wave equation*, SIAM J. Num. Anal., 44 (2006), pp. 2408–2431.

[10] J. Hesthaven and T. Warburton, *Nodal high-order methods on unstructured grids: I. time-domain solution of Maxwell's equations*, J. Comput. Phys., 181 (2002), pp. 186–221.

[11] ———, *Nodal Discontinuous Galerkin Methods*, no. 54 in Texts in Applied Mathematics, Springer-Verlag, New York, 2008.

[12] X. Meng, C.-W. Shu, and B. Wu, *Optimal error estimates for discontinuous Galerkin methods based on upwind-biased fluxes for linear hyperbolic equations*, Math. Comp., (2015). To appear.

[13] P. Monk and G. Richter, *A discontinuous Galerkin method for linear symmetric hyperbolic systems in inhomogeneous media*, J. Sci. Comp., 22-23 (2005), pp. 443–477.

[14] B. Riviere and M. Wheeler, *Discontinuous finite element methods for acoustic and elastic wave problems*, Contemp. Math., 329 (2003), pp. 271–282.

[15] T. Warburton, *A low-storage curvilinear discontinuous Galerkin method for wave problems*, SIAM J. Sci. Comput., 35 (2013), pp. A1987–A2012.

[16] G. B. Whitham, *Linear and Nonlinear Waves*, Wiley-Interscience, New York, 1999.

[17] L. Wilcox, G. Stadler, C. Burstedde, and O. Ghattas, *A high-order discontinuous Galerkin method for wave propagation through coupled elastic–acoustic media*, J. Comput. Phys., 229 (2010), pp. 9373 – 9396.